Multi-Agent Combinatorial Path Finding with Heterogeneous Task Duration

Yuanhang Zhang, Xuemian Wu, Hesheng Wang, Zhongqiang Ren*

***Abstract*— Multi-Agent Combinatorial Path Finding (MCPF) seeks collision-free paths for multiple agents from their initial locations to destinations, visiting a set of intermediate target locations in the middle of the paths, while minimizing the sum of arrival times. While a few approaches have been developed to handle MCPF, most of them simply direct the agent to visit the targets without considering the task duration, i.e., the amount of time needed for an agent to execute the task (such as picking an item) at a target location. MCPF is NP-hard to solve to optimality, and the inclusion of task duration further complicates the problem. This paper investigates heterogeneous task duration, where the duration can be different with respect to both the agents and targets. We develop two methods, where the first method post-processes the paths planned by any MCPF planner to include the task duration and has no solution optimality guarantee; and the second method considers task duration during planning and is able to ensure solution optimality. The numerical and simulation results show that our methods can handle up to 20 agents and 50 targets in the presence of task duration, and can execute the paths subject to robot motion disturbance.**

I. Introduction

Multi-Agent Path Finding (MAPF) seeks a set of collision-free paths for multiple agents from their start to goal locations while minimizing the total arrival times. This paper considers a generalized problem of MAPF, called Multi-Agent Combinatorial Path Finding (MCPF), which further requires the agents to visits a set of intermediate target locations before reaching their goals. MAPF and MCPF arises in applications such as manufacturing and logistics. Consider a fleet of mobile robots in a factory that are tasked to unload finished parts from different machines. The robots share a cluttered workspace and need to find collision-free paths to visit all the machines as the intermediate targets before going to their destinations to store the parts. MCPF naturally arises in such settings to optimize the manufacturing plan. MCPF is challenging due to both the collision avoidance between agents as in MAPF, and target sequencing, i.e., solving Traveling Salesman Problems (TSPs) to find the allocation and visiting orders of targets for all agents. Both the TSP and the MAPF are NP-hard to solve to optimality [20], and so is MCPF.

Although a few approaches have been developed [1], [4], [9], [13]–[15], [18], [21] to handle MCPF and its variants recently, most of them ignores or simplifies the *task duration* at a target location, which is ubiquitous in practice and is the main focus of this paper. In other words, when a robot reaches a target to execute the task there, it takes time for the robot to finish the task, and during this period, the robot has to occupy that target location and thus blocks the paths of other agents. Additionally, when sequencing the targets, the task duration must be considered when solving the TSPs to optimally allocating the targets and finding the visiting order. Furthermore, task duration can be heterogeneous with respect to the agents and targets: different agents may take different duration for the task at the same target, and for the same agent, different targets may require different duration.

All authors are with Shanghai Jiao Tong University, China. (email: yuanhang0610@gmail.com; zhongqiang.ren@sjtu.edu.cn).

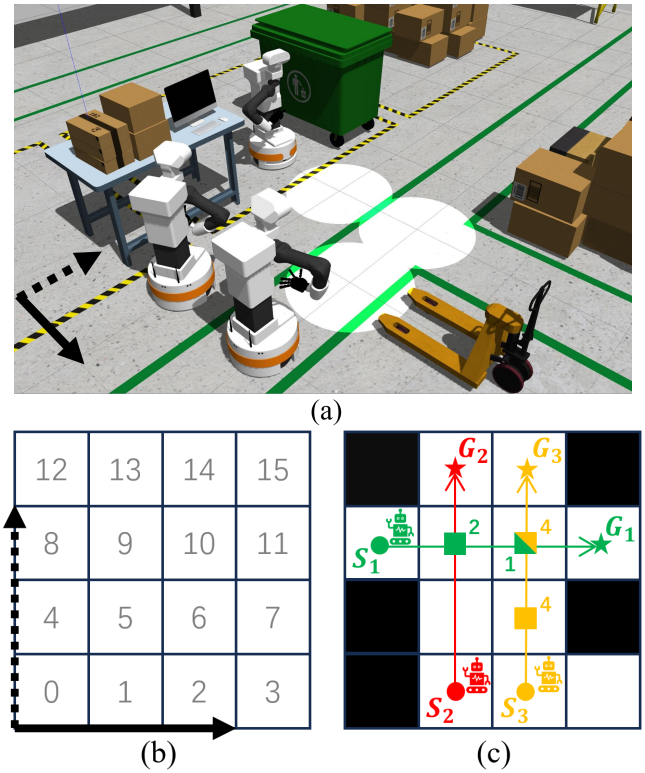

Fig. 1. A toy example of MCPF-D. The target locations with heterogeneous task duration are marked as the white disks in (a). (c) shows the a 4×4 grid representation of the workspace in (a) and each cell is encoded with a number as shown in (b). There are three targets 6, 9, 10, which are marked as square in (c). The color of the targets in (c) shows the assignment constraints. For instance, the task at target 10 can only be executed by the green agent with task duration 1, or by the yellow agent with task duration 4. The S and G shows the initial and goal locations of the agents.

To handle task duration, this paper first formulates a new problem variant of MCPF called MCPF-D, where D stands for heterogeneous task duration (Fig. 1). MCPF-D generalizes MCPF and is therefore NP-hard to solve to optimality. We then develop two methods to solve MCPF-D.

The first method has no solution optimality guarantee. It begins by ignoring the task duration and using an existing planner for MCPF (such as [15]) to find a set of paths,

and then post-processes the paths to incorporate the task duration while avoiding collision among the agents. The post-processing leverages [4] to build a temporal planning graph (TPG) that captures the precedence requirement between the waypoints along the agents' paths, and then add the task duration to the target locations while maintaining the precedence requirement to avoid agent-agent collision. While being able to take advantage of any existing planner for MCPF, this first method only finds a sub-optimal solution to MCPF-D and the solution cost can be far away from the true optimum especially in the presence of large task duration. We instantiate this method by using CBSS as the MCPF planner and name the resulting algorithm CBSS-TPG.

To find an optimal solution for MCPF-D, we develop our second method called Conflict-Based Steiner Search with Task Duration (CBSS-D), which is similar to CBSS [15] by interleaving target sequencing and path planning. CBSS-D considers task duration during planning, and CBSS-D differs from CBSS as follows. First, CBSS-D solves TSPs with task duration to find optimal target sequences for the agents to visit, and thus modifies the target sequencing part in CBSS. Second, when an agent-agent collision is detected during path planning, CBSS-D introduces a new branching rule, which is based on the task duration, to resolve the collision more efficiently than using the basic branching rule in CBSS.

We test and compare our two approaches using an online dataset [17]. As shown by our results, both CBSS-TPG and CBSS-D can handle up to 20 agents and 50 targets, and the solution cost returned by CBSS-D is up to 20% cheaper than CBSS-TPG especially when the task duration is large. Furthermore, the new branching rule in CBSS-D is able to help avoid up to 80% of the planning iterations needed for collision resolution in comparison with the regular branching rule in CBSS. Finally, we combine CBSS-D and TPG to both find high quality paths and execute the paths on robots with motion disturbance or inaccurate task duration, which is validated by our high-fidelity simulation in Gazebo.

II. Problem Formulation

Let index set $I = \{1, 2, \dots, N\}$ denote a set of N agents. All agents move in a shared workspace represented as an finite undirected graph $G = (V, E)$, where the vertex set V represents the possible locations for agents and the edge set $E \subseteq V \times V$ denotes the set of all possible actions that can move an agent between two vertices in V. An edge between $u, v \in V$ is denoted as $(u, v) \in E$, and the cost of an edge $e \in E$ is a positive real number $cost(e) \in (0, \infty)$. To simplify the problem, we consider the case where each edge has a unit cost, which is equal to the traversal time of that edge.

We use a superscript $i \in I$ over a variable to represent the agent to which the variable relates (e.g., $v^i \in V$ means a vertex related to agent i). The start (i.e., initial vertex) of agent i is expressed as $v_o^i \in V$, and $V_o \in V$ denotes the set of the starts of all agents. There are N destination vertices in G denoted by the set $V_d \subseteq V$. The destination vertices are also called goal vertices. In addition, let $V_t \subseteq V \backslash \{V_o \cup V_d\}$ denote the set of M (intermediate) target vertices. Each target or destination vertex $v \in V_t \cup V_d$ is associated with a task that must be executed by an agent. For each $v \in V_t \cup V_d$, let $f_A(v) \subseteq I$ denote the subset of agents that are capable to visit v and execute the task at v. Specifically, for each $v \in V_t \cup V_d$, let *task duration* $\tau^i(v)$, a non-negative integer, denote the amount of time that agent $i \in f_A(v)$ takes to execute the task at v. For the same vertex $v \in V_t \cup V_d$, different agents may take different amount of time to execute the task, and hence heterogeneous task duration. Any agent $i \in I$ (including $i \notin f_A(v)$) can occupy v along its path without executing the task at $v \in V_t \cup V_d$.

All agents share a global clock. An agent i has three possible actions a^i: move through an edge, wait in the current vertex, or execute the task if the agent is at $v \in V_t \cup V_d$. Here, both move and wait take a unit time and executing the task takes the amount of time indicated by the task duration. The cost of an action $cost(a^i)$ is the amount of time taken by that action. Let $\pi^i(v_1^i, v_k^i) := (a_1^i, a_2^i, \dots, a_\ell^i)$ denote a path for agent i between vertices v_1^i and v_k^i in G, where $a_k^i, k = 1, 2, \dots, \ell$ denote an action of the agent. Let $g(\pi^i(v_1^i, v_k^i))$ denote the cost of the path, which is the sum of the costs of all the actions taken by the agent in the path: $g(\pi^i(v_1^i, v_k^i)) = \sum_{k=1,2,\dots,\ell-1} cost(a_k^i)$.

Any two agents $i, j \in I$ are in conflict for any of the following two cases. The first case is an *edge conflict* (i, j, e, t), where two agents $i, j \in I$ go through the same edge e from opposite directions between times t and $t + 1$. The second case is a *vertex conflict* (i, j, v, t), where two agents $i, j \in I$ occupy the same vertex v at the same time t. Note that due to task duration, vertex conflicts include the case where an agent $i \in I$ is executing a task at some $v \in V_t \cup V_d$ within the time range $[t, t + \tau^i(v)]$, and another agent $j \in I, j \neq i$ occupies v at some time $t' \in [t, t+\tau^i(v)]$.

The MCPF-D problem aims to find a set of conflict-free paths for the agents such that: (i) the task at any $v \in V_t \cup V_d$ is executed by an eligible agent $i \in f_A(v)$; (ii) each agent $i \in I$ starts its path from v_o^i and ends at a unique goal $u \in V_d$ such that $i \in f_A(u)$; (iii) the sum of the path cost of all agents reaches the minimum.

Remark 1: When $\tau^i(v) = 0$ for all $v \in V_t \cup V_d, i \in f_A(v)$, MCPF-D becomes the existing MCPF problem [15]. Here, a path π^i is represented by a list of actions of agent i, and such a π^i can always to converted to a list of vertices $\pi^i = (v_1^i, v_2^i, \dots, v_k^i)$ (not vice versa), where the subscripts indicate the consecutive time steps and the vertices indicate the locations of the agent at the corresponding time steps. For the rest of this paper, we use both representation interchangeably.

III. Preliminaries

A. Conflict-Based Steiner Search

1) Overview: [15] for MCPF is shown in Alg. 1,[1] which interleaves target sequencing and path planning as

[1]In Alg. 1, Line 2 and 12 are marked in blue indicating the differences between CBSS and CBSS-D, which will be explained in Sec. V.

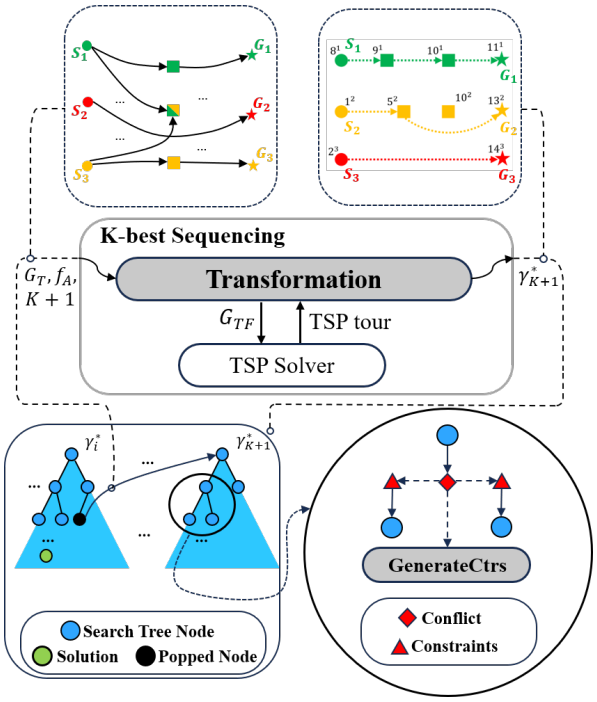

Fig. 2. An illustration of CBSS and CBSS-D. Both of them generate K-best target sequences and leverage CBS to resolve conflicts between agents. The differences between them are represented by the transformation and constraints generation, which are highlighted by gray-filled text boxes.

follows (Fig. 2). CBSS creates a complete undirected target graph $G_T = (V_T, E_T, C_T)$ with the vertex set $V_T = Vo \bigcup Vt \bigcup Vd (|V_T| = 2N + M)$ and edge set E_T (Line 1). Here, C_T represents a symmetric cost matrix of size $(2N + M) \times (2N + M)$ that defines the cost of each edge in E_T, which is the minimal path cost between the two vertices in the workspace graph G. CBSS then ignores any conflict between the agents and solve a mTSP on G_T to find target sequences that specify the allocation and visiting order of the targets for each agent (Line 2, Sec. III-A.2). Next, CBSS fixes the target sequence, plans the corresponding paths, and then resolves conflicts along the paths by using Conflict-Based Search (Line 3-17, Sec. III-A.3). Finally, CBSS alternates between resolving conflicts along paths and generating new target sequences until an optimal solution is found.

2) K-best joint sequences: To generate new target sequences, CBSS solves a K-best TSP, which requires finding a set of K cheapest target sequences. Specifically, let $\gamma^i = \{v^i_0, u^i_1, u^i_2, ..., u^i_l, v^i_d\}$ denote a *target sequence* visited by agent $i \in I$, where v^i_0 is the start of agent i, u^i_j is the j-th target visited by agent i with $j = 1, ..., l$ and $v^i_d \in V_d$ is the goal of agent i. Let $\gamma = \{\gamma^i : i \in I\}$ denote a *joint (target) sequence*, which is a collection of target sequences of all agents. The cost of a joint sequence is defined as $cost(\gamma) := \sum_{i \in I} cost(\gamma^i)$, where the cost between any two targets $u, v \in \gamma^i$ is set to be the minimum path cost from u to v in G. Here, CBSS seeks a set of K-best joint sequences $\gamma_1, \gamma_2, ..., \gamma_k$, whose costs are monotonically non-decreasing: $cost(\gamma^*_1) \leq cost(\gamma^*_2) \leq ... \leq cost(\gamma^*_k)$.

Algorithm 1 Pseudocode for CBSS (CBSS-D)

1: $G_T = (V_T, E_T, C_T) \leftarrow$ ComputeGraph(G)
2: $\gamma^*_1 \leftarrow$ *K-best-Sequencing*($G_T, f_A, K = 1$)
3: $\Omega \leftarrow \emptyset$
4: $\pi, g \leftarrow$ *LowLevelPlan*(γ^*_1, Ω)
5: Add $P_{root,1} = (\pi, g, \Omega)$ to OPEN
6: **while** OPEN is not empty **do**
7: $P_l = (\pi_l, g_l, \Omega_l) \leftarrow$ OPEN.pop()
8: $P_k = (\pi_k, g_k, \Omega_k) \leftarrow$ *CheckNewRoot*(P_l, OPEN)
9: $cft \leftarrow$ *DetectConflict*(π_k)
10: **if** $cft = NULL$ **then**
11: **return** π_k
12: $\Omega \leftarrow$ *GenerateConstraints*(cft)
13: **for all** $\omega^i \in \Omega$ **do**
14: $\Omega'_k = \Omega_k \cup \{\omega^i\}$
15: $\pi'_k, g'_k \leftarrow$ *LowLevelPlan*($\gamma(P_k)$, Ω'_k)
16: // In this LowLevelPlan, only agent i's path is planned.
17: Add $P'_k = (\pi'_k, g'_k, \Omega'_k)$ to OPEN
18: **return** failure

To find K-best joint sequences, CBSS first leverages a transformation method in [7] to convert a mTSP to an equivalent (single agent) TSP so that the existing TSP solver (such as LKH [3]) can be used. The resulting solution to the TSP can then be un-transformed to obtain the joint sequence to the original mTSP. Additionally, to find K-best joint sequences, CBSS leverages a partition method [2], [19], which iteratively creates new TSPs in a systematic way based on the first $(K-1)$-best joint sequences, obtains an optimal solution to each of the new TSPs, and picks the cheapest solution as the K-th best solution.

3) Conflict Resolution: For each joint sequence, CBSS uses CBS, a two-level search that creates a search tree, to resolve conflicts and plan paths. Each node P in a tree is defined as a tuple of (π, g, Ω), where: $\pi = (\pi^1, \pi^2, ..., \pi^N)$ is a joint path, a collection of all agents' paths; g is the scalar cost value of π, i.e., $g = g(\pi) = \sum_{i \in I} g(\pi^i)$; and Ω is a set of (path) constraints,[2] each of which is (i, v, t) (or (i, e, t)) and indicates that agent i is forbidden to occupy vertex v (or traverse edge e) at time t.

We first describe CBSS when there is only one joint sequence and then describe when to generate new joint sequences. With the first computed joint sequence γ^*_1, a joint path π_1 is planned by running some low-level (single-agent) planner such as A^* for each agent, while visiting the targets in the same order as in γ^*_1. Then, a node corresponding to γ^*_1 is created, which becomes the root node of the first tree. If no conflict is detected between agents in π_1, the search terminates and return π_1, which is an optimal solution to MCPF. Otherwise (i.e., π_1 has a conflict, say(i, j, v, t)), then two new constraints (i, v, t) and (j, v, t) are created as in CBS [16]. For each new constraint (say (i, v, t)), the low-level planner is invoked for agent i to find a minimum-cost path that satisfies all constraints that have been imposed on agent i, and follows the same target sequence as in γ^*_1. Then, a corresponding node is generated and added to OPEN,

[2]For the rest of this article, we refer to path constraints simply as constraints, which differs from the aforementioned assignment constraint.

where OPEN is a queue that prioritizes nodes based on their g-values from the minimum to the maximum. In the next search iteration, a node with the minimum cost is popped from OPEN for conflict detection and resolution again. The entire search terminates until a node with conflict-free joint path is popped from OPEN, which is returned as the solution.

CBSS generates new joint sequences when needed during this search process. When a node $P = (\pi, g(\pi), \Omega)$ is popped from OPEN. If $g(\pi)$ is no larger than the cost of a next-best joint sequence (say $cost(\gamma_2^*)$), then, the search continues to detect and resolve conflict as aforementioned. Otherwise (i.e., $g(\pi) > \gamma_2^*$), a new (root) node (of a new tree) is created, where paths of agents are planned based on γ_2^*. Then, the same conflict detection and resolution process follows. Note that since $cost(\gamma_1^*)$ is a lower bound to the optimal solution cost of MCPF, and that the nodes are systematically generated and expanded in a best-first search manner, CBSS finds an optimal solution to the MCPF [15].

B. Temporal Plan Graph

To handle kinematic constraints of robots, Temporal Plan Graph (TPG) [5] was developed to post-process the joint path output by a MAPF (or MCPF) planner. TPG converts a joint path to a directed acyclic graph $\mathcal{G} = (\mathcal{V}, \mathcal{E})$, where each vertex $s \in \mathcal{V}$ represents an event[3] that an agent enters a location, and each directed edge $e = (s, s^{'}) \in \mathcal{E}$ indicates a temporal precedence between events: event s' happen after event s. There are two types of edges in $\mathcal{G}$ and the intuition can be described as follows. Given a conflict-free joint path $\pi = (\pi^1, \pi^2, \ldots, \pi^N)$ output by a MAPF planner.

- Type 1: Each agent $i \in I$ enters locations in the same order given by its path π^i;
- Type 2: Any two agents $i, j \in I, i \neq j$ enter the same location in the same order as in their paths π^i and π^j.

Let $\pi^i = (v_0^i, v_1^i, ..., v_T^i)$ denote agent i's path in π, where s_t^i denotes the location agent i reaches at time t. Let T denote the largest arrival time among all agents, and for those agents that arrive at their goals before T, their paths are prolonged by letting them wait at their goals until T. A TPG is then constructs as follows. To create vertices and Type 1 edges in TPG, for each agent i, we extract a route r^i from path π^i by removing the wait actions (i.e., keeping only the first of the consecutive identical locations in π^i). All locations in the routes $r^1, r^2, ..., r^N$ constitute the vertices of TPG, denoted by s_t^i with $i \in I$ and $t \in [0, T]$ indicating that agent i occupies location v_t^i at time t. For each pair of two consecutive vertices s_t^i and $s_{t'}^i$ in the route r^i, a Type 1 edge $(s_t^i, s_{t'}^i)$ is created, indicating that agent i enters s_t^i before entering $s_{t'}^i$. For each pair of two identical locations $s_t^i = s_{t'}^j$ on two different routes ($i \neq j$) with $t < t'$, a Type 2 edge $(s_t^i, s_{t'}^j)$ is created, indicating that agent i enters s_t^i before agent j enters $s_{t'}^j$.

The resulting TPG encodes the precedence requirement that ensures the collision-free execution of the joint path π. In [5], a TPG is used to handle the kinematic constraints of the robots to ensure robust execution of the paths, while in this paper, we use TPG, combined with CBSS, as our first method to handle task duration in MCPF-D, which is presented next.

[3] s denotes a vertex in $\mathcal{G}$ and v denotes a vertex in G.

IV. CBSS-TPG

A. Algorithm Description

CBSS-TPG begins by ignoring all task duration (i.e., set all task duration to 0), which yields a MCPF problem. Then CBSS is applied to obtain a conflict-free joint path for this MCPF problem, denoted by $\pi_a = (\pi_a^1, \pi_a^2, ..., \pi_a^N)$. Then, we propose TPG-D to post-process the joint path π_a by incorporating the task duration and avoid additional conflicts brought by the task duration, explained in Sec. IV-B.

Remark 2: After the first step in CBSS-TPG where a joint path is obtained, the remaining problem is how to incorporate the task duration into that joint path while avoiding conflicts. A naive approach is, along the joint path π_a, let an agent i stay at a target vertex v until the task at v is finished. Meanwhile, let all other agents wait at their current vertex until agent i finishes the task, and then let all other agents start to move again. This naive method would lead to many unnecessary wait actions. We therefore develop TPG-D, which is able to identify a small subset of agents that are affected by a task, and only let these affected agents wait until that task is finished.

B. TPG Post-Process

Our method TPG-D (Alg. 2) takes as input a joint path π output by CBSS, task duration τ and a TPG $\mathcal{G}$ that is constructed by the method in [5], and returns conflict-free joint path π_c with the task duration incorporated. TPG-D is based on the following property of TPG: Recall that the directed edges in $\mathcal{G}$ indicates the precedence between events. When an event happens (i.e., an agent has reached a location s_t^i), both s_t^i and all out-going edges of s_t^i can be deleted from $\mathcal{G}$ to remove the corresponding precedence constraints. Then, an event has no precedence constraint (and can take place) if the corresponding vertex s_t^i has zero in-degree in $\mathcal{G}$.

Based on this property, TPG-D further introduces *duration value* $D(s_t^i)$ for each vertex $s_t^i \in \mathcal{V}$ to handle task duration, where $D(s_t^i)$ represents the time agent i should spend at location s_t^i. Here, $D(s_t^i)$ includes both the waiting time (if any) and the task duration of agent i at s_t^i. TPG-D is an iterative algorithm, and in any iteration, let L_0 denote the list of vertices in $\mathcal{G}$ with zero in-degree, and let L_d denote a list of vertices to be deleted in $\mathcal{G}$.

At the beginning, TPG-D initializes π_c (the joint path to be returned) with $\emptyset$ and v_c (the current joint vertex of all agents) with the starting vertices of all agents (Line 3-4). TPG-D initializes $D(s_t^i)$ for all $s_t^i \in \mathcal{G}$ by finding the waiting time and the task duration at s_t^i based on π_a and τ. If there is no wait or no task duration related to s_t^i, procedures WaitTime and TaskDuration simply return zero and $D(s_t^i) = 0$.

In each iteration (Line 6-19), TPG-D first finds the set L_0 of all vertices with zero in-degree in $\mathcal{G}$ (Line 7). Then, for each vertex s_t^i in L_0, TPG-D reduces its D-value by one

Algorithm 2 Pseudocode for TPG-D

1: **Input**: A TPG $\mathcal{G}$, a joint path π output by CBSS, and all task duration τ.
2: **Output**: A conflict-free joint path π_c where each agent follows the same visiting order in $\mathcal{G}$
3: $\pi_c \leftarrow (\emptyset, \emptyset, ..., \emptyset)$
4: $v_c \leftarrow (v_0^0, v_0^1, ..., v_0^N)$
5: $D(s_t^i) \leftarrow$ WaitTime(v_t^i, π) + TaskDuration(v_t^i,π,τ)
6: **while** $\mathcal{G} \neq \emptyset$ **do**
7: $L_0 \leftarrow$ *ZeroInDegVertices*($\mathcal{G}$)
8: $L_d \leftarrow \emptyset$
9: **for all** $s_t^j \in L_0$ **do**
10: $v_c^j \leftarrow s_t^j$
11: **if** $D(s_t^j) > 0$ **then**
12: $D(s_t^j) = D(s_t^j) - 1$
13: **for all** $s_t^j \in L_0$ **do**
14: **if** *CheckDelete*(s_t^j) **then**
15: Add s_t^j to L_d
16: Delete all $s \in L_d$ from $\mathcal{G}$
17: **for all** $i \leftarrow 1$ **to** N **do**
18: **if** Agent i has not reached the end of π^i **then**
19: Append v_c^i to the end of π_c^i
20: **return** π_c ▷ Final conflict-free joint path

unless $D(s_t^i)$ is already zero. Then, TPG-D finds all s_t^i in L_0 that should be deleted from $\mathcal{G}$ (Line 13-15) via procedure CheckDelete and add them into L_d. CheckDelete can be implemented in different ways [5], [6] and we consider the following three conditions when a vertex s_t^i can be deleted: (i) the in-degree of s_t^i is zero; (ii) $D(s_t^i) = 0$ and (iii) the agent can reach the next vertex s_{t+1}^i without colliding with any other agents. Here, (iii) is needed since another agent j may stay at vertex $s_{t'}^j = s_{t+1}^i$ for task execution, and if agent i leaves s_t^i, i cannot reach s_{t+1}^i. Then, TPG-D deletes all vertices in L_d from $\mathcal{G}$ and append $v_c^i \in v_c$ (the current vertex of each agent) to the end of π_c^i for each $i \in I$, if i has not reached its goal yet. In the next iteration, since vertices in L_d are deleted from $\mathcal{G}$, L_0 will change and v_c will be updated correspondingly. TPG-D terminates when $\mathcal{G}$ is empty, which means all agents have reached their goals (Line 6).

Example 1: For the example in Fig. 1, after invoking CBSS, the resulting joint sequence is $\gamma^1 = (8, 9, 10, 11)$, $\gamma^2 = (1, 13)$, $\gamma^3 = (2, 6, 14)$ and the resulting joint path is $\pi_a^1 = (8, 9, 10, 11)$, $\pi_a^2 = (1, 5, 9, 13)$, $\pi_a^3 = (2, 6, 6, 10, 14)$). If one simply add the task duration back to π_a, the resulting joint path $\pi_b^0 = ((8, 9, 9, 9, 10, 10, 11)$, $\pi_b^1 = (1, 5, 9, 13)$, $\pi_b^2 = (2, 6, 6, 6, 6, 6, 6, 10, 14)$ is not conflict-free. Fig. 3 shows the constructed TPG by the method in [5] and the blue number on the upper right corner of each circle in Fig. 3 shows the D-value introduced by our TPG-D. The returned joint path by TPG-D is $\pi_c^0 = (8, 9, 9, 9, 10, 10, 11)$, $\pi_c^1 = (1, 5, 5, 5, 9, 13)$, $\pi_c^2 = (2, 6, 6, 6, 6, 6, 6, 10, 14))$, which is conflict-free.

C. Properties

We say a joint path π_1 follow the same visiting order as π_2, if the following conditions hold: (i) every vertex that appears in π_1^i also appear in π_2^i for all $i \in I$; (ii) if vertex u appears after v in π_1^i, then u also appears after v in π_2^i for all $i \in I$; (iii) if a vertex v appears in two agents' paths $\pi_1^i, \pi_1^j, i \neq j$ and j visits v after i has visited v, then j also visits v after i has visited v in π_2^i, π_2^j. Note that two joint paths with the same visiting order may differ due to variations in the waiting periods experienced by some agents along each path.

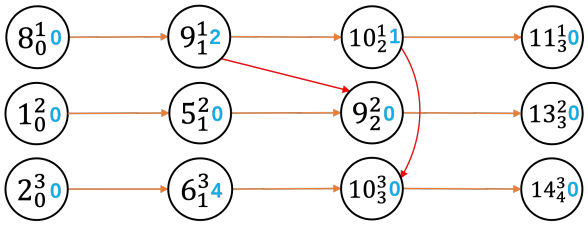

Fig. 3. TPG of the example in Fig. 1. Vertex s_t^i means agent i moves to location s at time t, and the number in blue is the value of $D(s_t^i)$. The orange arrows represent Type 1 edges and the red arrows represent Type 2 edges.

The construction of the TPG $\mathcal{G}$ captures the precedence between the agents in π using Type 1 and Type 2 edges [5]. The π_c returned by TPG-D preserves the precedence in π by iteratively deleting and appending the zero in-degree vertices (via *CheckDelete*) to the returned joint path. By enforcing the precedence, π_c follows the same visiting order as π. We summarize this property in the following theorem.

Theorem 1: Let π, τ and $\mathcal{G}$ denote the input to TPG-D. Then, π_c returned by TPG-D follows the same visiting order as π.

Theorem 1 ensures that all agents eventually reach their respective goals along π_c. Additionally, the third condition in *CheckDelete* in TPG-D ensures that an agent does not move to its next vertex along its path unless the agent can reach it without conflict. Therefore, we have the following theorem.

Theorem 2: The joint path π_c generated by TPG-D is conflict-free solution to MCPF-D.

CBSS-TPG can't guarantee the optimality of the returned solution π_c. Next, we will introduce our second method CBSS-D which finds an optimal solution for MCPF-D.

V. CBSS-D

There are two main differences between CBSS-D and CBSS: First, CBSS-D modifies the transformation method for target sequencing to handle task duration (Sec. V-A); Second, when a conflict is detected, CBSS-D introduces a new branching rule, which leverages the knowledge of task duration, to resolve the conflict more efficiently than using the basic branching rule in CBSS (Sec. V-B).

A. Transformation for Sequencing

As aforementioned, to find K-best joint sequences, CBSS first leverages a transformation method to convert a mTSP to an equivalent (single agent) TSP, then uses a partition method to solve a K-best (single agent) TSP, and then un-transform each of the obtained K-best (single agent) tours to a joint sequence. Here, CBSS-D only modifies the transformation method while the partition method remains the same.

The transformation method first creates a transformed graph G_{TF} out of the target graph G_T by defining the vertex

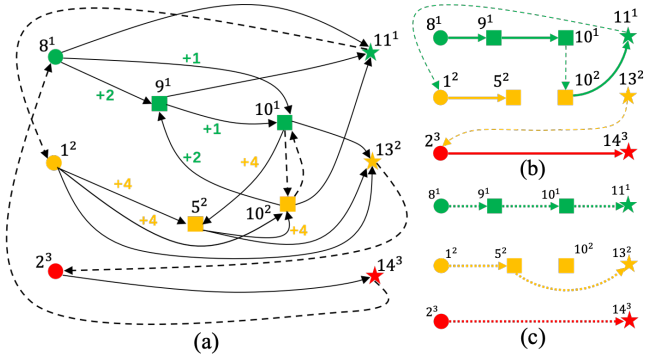

Fig. 4. The transformation method for the toy example in Fig. 1. Here, (a) shows the transformed graph G_{TF}. The cost related to task duration is denoted by $+x$, where x is the corresponding task duration. (b) shows the TSP tour in G_{TF} computed by a TSP solver. (c) shows the joint sequence untransformed from the TSP tour.

set V_{TF} as $V_{TF} := V_0 \bigcup U$, where U is an augmented set of targets and goals: for each $v \in V_t \bigcup V_d$, a copy of v^i of v for agent i is created if $i \in f_A(v)$. Making these copies of each target v for agents in $f_A(v)$ help handle the assignment constraints [15]. The edges E_{TF} and their corresponding costs C_{TF} are set in a way such that an optimal solution tour in G_{TF} has the features that allow the reconstruction of a joint sequence out of the tour. In short, (i) when an optimal tour visits the goal of agent i, the tour will visit the initial vertex of the next agent $i+1$. This allows breaking the tour into multiple sub-tours based on the goals during the reconstruction (Fig. 4(b)), and each sub-tour becomes a target sequence of an agent in the resulting joint sequence. (ii) When an optimal solution tour in G_{TF} visits a copy of targets or destination v, the tour will immediately visit all other copies of v before visiting a next target. When reconstructing the joint sequence, only the first copy of a target is kept, which identifies the agent that is assigned to this target, and all other subsequent copies are removed during the reconstruction of a joint sequence (Fig. 4(c)).

For each target or goal $v \in V_t \bigcup V_d$, a copy of v^i of v for agent i is created if $i \in f_A(v)$. To include task duration, the new part in CBSS-D is that, it adds an additional cost $\tau^i(v)$ for the in-coming edge that goes into v^i, where $\tau^i(v)$ is the task duration. Note that although the task duration is defined on vertices, we are able to add the task duration to a corresponding edge because there is a one-one correspondence between each target and an in-coming edge. For the same target, different agents may have different duration, which is also allowed here, since for every target, there is a unique in-coming edge for each agent. The property of the transformation method in CBSS-D is summarized with the following theorem. The proof in [10] and [15] can be easily adapted.

Theorem 3: For a MCPF-D Problem, given G_T, f_A and τ, the transformation method computes a minimum cost joint sequence that visits all targets and ends at goals while satisfying all assignment constraints.

Example 2: For the problem in Fig. 1, as shown in Fig. 4, the generated joint sequence by our transformation method is $\gamma = \{(8, 9, 10, 11), (1, 13), (2, 6, 14)\}$.

Algorithm 3 Pseudocode for GenerateConstraints

1: **Input**: A vertex or edge conflict *cft*
2: **Output**: The generated constraints Ω
3: $\Omega \leftarrow \emptyset; \omega_1 \leftarrow \emptyset; \omega_2 \leftarrow \emptyset$
4: **if** *cft* is an edge conflict **then**
5: $\quad \omega_1 = \{(i, e, t)\}$; $\omega_2 = \{(j, e, t)\}$
6: **else if** *CheckExecution*(i) **then**
7: $\quad t_s, t_e =$ *TaskStartEnd*(i, v, t)
8: $\quad \omega_1 = \{(i, v, t_1) | t_s \leq t_1 \leq t\}$
9: $\quad \omega_2 = \{(i, j, t_2) | t \leq t_2 \leq t_e\}$
10: **else if** *CheckExecution*(j) **then**
11: $\quad t_s, t_e =$ *TaskStartEnd*(j, v, t)
12: $\quad \omega_1 = \{(i, v, t_1) | t \leq t_1 \leq t_e\}$
13: $\quad \omega_2 = \{(i, v, t_2) | t_s \leq t_2 \leq t\}$
14: **else**
15: $\quad \omega_1 = \{(i, v, t)\}$; $\omega_2 = \{(j, v, t)\}$
16: $\Omega \leftarrow \{\omega_1, \omega_2\}$
17: **return** Ω

B. Different Branching Rules

Naively applying the conflict resolution method in CBSS to MCPF-D can lead to inefficient computation. For example: when a vertex conflict (i, j, v, t) is detected in an iteration of CBSS, two constraints (i, v, t) and (j, v, t) are created and leads to two new branches. Say i executes the task at target v during time $[t, t+\tau^i(v)]$. Then, the branch with the constraint (j, v, t) replans the path for agent j. Along the replanned path, agent j may enter v at time $t+1$, which is still in conflict with agent i if $t+1 \in [t, t+\tau^i(v)]$. This branch thus requires another iteration of conflict resolution. When $\tau^i(v)$ is large, it can lead to many iterations of conflict resolution and thus slow down the computation. Our new branching rule seeks to resolve multiple conflicts related to the same task in one iteration and therefore saves computational effort.

We modify the function *GenerateConstraints* on Line12 in Alg. 1, and the modified branching rule is shown in Alg. 3. For an edge conflict (i, j, e, t), agent i and j must not be executing any task, so CBSS-D resolves the conflict in the same way as CBSS by generating two constraints (i, e, t) and (j, e, t). For a vertex conflict (i, j, v, t), agent i and j can not be simultaneously executing tasks at target v at time t. Therefore, there are three cases to be considered:

- First, if *CheckExecution* finds agent i is executing task at vertex v, two *sets of constraints* are generated. The first set is $\{(i, v, t_1) | t_s \leq t_1 \leq t\}$ where t_s is the time that agent i starts the task at v. The second set of constraints is $\{(j, v, t_2) | t \leq t_2 \leq t_e\}$ where t_e is the time that agent i ends the task at v (Line 6-9).
- Second, if *CheckExecution* finds agent j is executing task at v, two sets of constraints are generated in a similar way (Line 10-13).
- If none of the agents are executing task at v, two constraints (i, v, t) and (j, v, t) are generated in the same way as in CBSS (Line 14-15).

We discuss the idea behind this branching rule in Sec. V-C.

Example 3: In Fig. 1, there is a vertex conflict $(i = 1, j = 2, v = 9, t = 1)$. When using the branching rule in CBSS to

resolve this conflict, additional vertex conflicts $(i = 1, j = 2, v = 9, t = 2), (i = 1, j = 2, v = 9, t = 3)$ will be detected and resolved in the subsequent iterations. When using our new branching rule, the conflict $(i = 1, j = 2, v = 9, t = 1)$ can be resolved in only one iteration.

Example 4: Here we provide a comparison between the solutions returned by CBSS-TPG and CBSS-D for the toy problem in Fig. 1. CBSS-TPG returns $\pi_c^0 = ((8, 9, 9, 9, 10, 10, 11)$, $\pi_c^1 = (1, 5, 5, 5, 9, 13)$, $\pi_c^2 = (2, 6, 6, 6, 6, 6, 6, 10, 14))$ with the cost of 19. CBSS-D returns $\pi_*^0 = ((8, 9, 9, 9, 10, 10, 11)$, $\pi_*^1 = (1, 5, 5, 5, 9, 13)$, $\pi_*^2 = (2, 6, 6, 6, 6, 6, 10, 14))$ with the cost of 18 which is the optimal cost. One can expect larger cost difference when the task duration becomes larger.

C. Solution Optimality of CBSS-D

We first present the property of our new branching rule and then use it to show the solution optimality of CBSS-D.

Definition 1 (Mutually Disjunctive Constraints): Two vertex or edge constraints for agents i and j are mutually disjunctive [8], if there does not exist a conflict-free joint path such that both constraints are violated. Besides, two sets of constraints corresponding to agent i and j are mutually disjunctive if every constraint in one set is mutually disjunctive with every constraint in the other set.

Theorem 4: For any conflict, the branching rule in Sec. V-B generates two mutually disjunctive constraint sets C_1 and C_2.

Proof: If the conflict between i and j is an edge or vertex conflict and none of the agents execute a task in v, the constraints are generated in the same way as CBS and are thus mutually disjunctive [8]. Otherwise, consider the two sets C_1, C_2 of constraints generated in Alg. 3. We prove that C_1 and C_2 are mutually disjunctive by contradiction. Assuming that C_1 and C_2 are not mutually disjunctive, then there must exist at least one conflict-free joint path π' that violates at least one constraint in C_1 and at least one constraint in C_2. Then, i and j are in conflict along π', which leads to contradiction. ∎

With Theorem 3 4, the proof in [15] can be readily adapted to show that the solution returned by CBSS-D is optimal for MCPF-D. First, the transformation method in Sec. V-A (Theorem 3) and the partition method in [2], [15], [19] finds K-best joint sequences for a given K. For each of those joint sequences, CBSS-D uses CBS-like search to resolve conflicts, and Theorem 4 ensures that the search with the new branching rule can find a conflict-free joint path if one exists. Finally, CBSS-D is same as CBSS [15] when generating new joint sequences and resolving conflicts, by using an OPEN list to prioritize all candidate nodes based on their g-costs and always select the minimum-cost one for processing. The returned solution is thus guaranteed to be a conflict-free joint path with the minimum-cost. We thus have the following theorem.

Theorem 5: For a solvable MCPF-D problem (i.e., the problem has at least one conflict-free joint path), CBSS-D terminates in finite time and returns an optimal solution.

VI. Results

A. Test Settings

We implement both CBSS-TPG and CBSS-D in Python and use LKH-2.0.10 as the TSP solver.[4] Similarly to [15], we use SIPP [12] as the low-level planner in a space-time graph $G \times \{0, 1, 2, ..., T\}$ subject to vertex and edge constraints. We select two maps of different sizes from a online data set[5] and generate a four-connected grid-like graph G from each of the maps. This data set also includes 25 test instances for each map, where each instance includes hundreds of start-goal pairs. For each case, we use the first start-goal pair as the v_o and v_d for the robot and select randomly from the rest of the goals as the target v_t. All tests run on a computer with an Intel Core i9-13900K CPU and 64 GB RAM. Each test instance has a runtime limit of 1 minute and ϵ, a hyper-parameter in CBSS [15] that allows for bounded sub-optimal solutions, is always set to be zero. Recall that, N, M are the number of agents and targets respectively and the number of destinations are not included in M.

Since there many variations of MCPF-D by selecting different f_A and τ, it is impossible to evaluate all of them. We select three representative scenarios:

- (Scene 1) All targets are anonymous (i.e., $f_A(v) = I, \forall v \in V_t \bigcup V_d \ and \ \tau^i(v) = \tau^j(v), \forall i, j \in f_A(v)$). Here, the transformation in CBSS-D can be simplified in the same way as discussed in [11], [14], [15]: There is no need to make copies of targets and destinations for each agent and the related edges can be deleted.
- (Scene 2) Every destination is assigned to a unique agent. Every target has two randomly chosen eligible agents, and the task duration of all targets stays the same for all eligible agents.
- (Scene 3) Similar to Scene 2, every destination is assigned to a unique agent and every target has two randomly chosen eligible agents. Additionally, every target has heterogeneous task duration for the eligible agents, which is a randomly sampled integer. The sampling ranges vary in different tests and will be elaborated later.

B. CBSS-D Versus CBSS-TPG

This section compares CBSS-D and CBSS-TPG in Scene 1 and 2 for $N \in \{10\}, M \in \{10, 20, 30, 40, 50\}$ and $\tau^i(v) \in \{2, 5, 10, 20\}$. We test with two maps, Random 32×32 and Maze 32×32. Fig. 5 and 6 report the corresponding success rates and cost ratios. The cost ratio is defined as:

$$cost\ ratio = \frac{cost(\pi_{CBSS-TPG}) - cost(\pi_{CBSS-D})}{cost(\pi_{CBSS-TPG})} \times 100\% \quad (1)$$

For the success rates, as shown in Fig. 5, first, the maze map is harder than the random map in general, where the agents are more likely to run into conflict with each other.

[4]LKH [3] (`http://akira.ruc.dk/~keld/research/LKH/`) is a heuristic algorithm for TSP, which does not guarantee solution optimality but often finds an optimal solution for large-scale TSP instances in practice. We use LKH due to its computational efficiency. Other TSP solvers can also be used.

[5]`https://movingai.com/benchmarks/mapf/index.html`

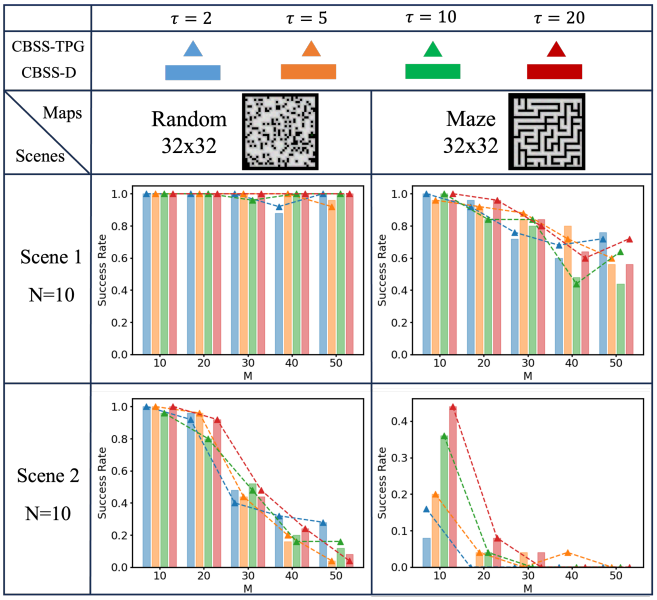

Fig. 5. The success rates of CBSS-TPG and CBSS-D with various number of targets M and task duration τ. The maze is harder than the random map in general and both algorithms achieve similar success rates.

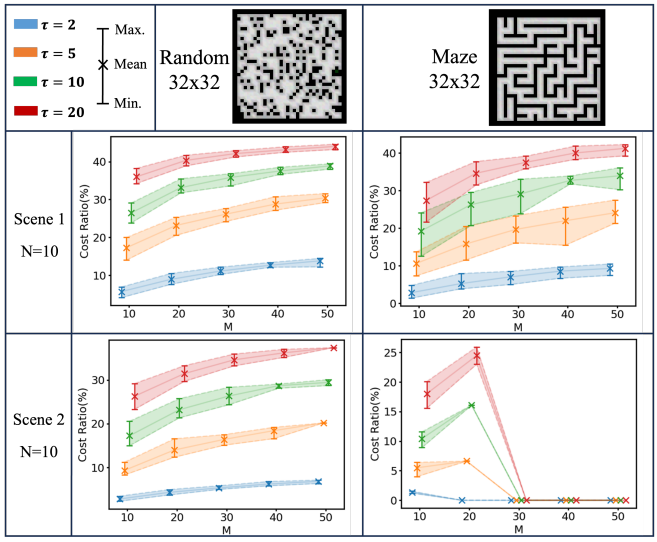

Fig. 6. The cost ratios of CBSS-TPG and CBSS-D. The vertical axis shows the percentage. In Scene 2 in the maze map, the cost ratio quickly goes down to zero because the corresponding success rate is almost zero. CBSS-D finds cheaper solution than CBSS-TPG especially when τ is large.

Maps and Test settings	Random 32x32 $M = \{10,20,30,40,50\}$ $\tau = \{2,5,10,20\}$	Maze 32x32 $M = \{10,20,30,40,50\}$ $\tau = \{2,5,10,20\}$
Number of instances with resolved conflicts and satisfying: $\boldsymbol{N_c^1}$ </>/= $\boldsymbol{N_c^2}$		
N=5	0/**4**/175	0/**4**/156
N=10	1/**13**/203	1/**6**/17
N=20	0/**3**/48	-/-/-
	Min./Mean/Max.	Conflict ratio (%)
N=5	40/**57.02**/**71.43**	4.55/**19.55**/40.00
N=10	-8.00/**31.11**/70.97	-11.43/**14.22**/33.33
N=20	8.38/**11.52**/14.48	-/-/-

Fig. 7. The number of resolved conflicts of CBSS-D with different branching rules. The new branching rule is able to reduce the number of conflicts resolved during planning.

Both planners have lower success rates in the maze map than the random map. Second, as M increases, the corresponding TSP is harder to solve and thus the success rates decrease. Most of the failed instances time out when solving a TSP problem. In addition, CBSS-D and CBSS-TPG have similar success rate in general.

For the cost ratios shown in Fig. 6, CBSS-D finds better (up to 40% cheaper) solutions than CBSS-TPG does, especially when τ is large. This is expected since CBSS-TPG does not consider task duration in planning and simply let the related agents wait till the other agents finish their task, while CBSS-D considers task duration during planning.

C. CBSS-D With Different Branching Rules

This section compares the number of conflicts resolved in CBSS-D by using different branching rules, namely the regular branching rule in CBSS [15] (denoted as old) and the new branching rule developed in this paper (denoted as new). We run the tests in Scene 2 since it is more challenging according to the results in the previous section. In addition to varying M and τ, we also vary the number of agents $N \in \{5, 10, 20\}$. For each N, we sum up the data for $M = \{10, 20, 30, 40, 50\}$ and $\tau = \{2, 5, 10, 20\}$ and thus there are 500 instances for each N. Let N_c^{old}, N_c^{new} denotes the number of resolved conflicts using old and new branching rules respectively.

As shown in Fig. 7, N_c^{new} is usually smaller than N_c^{old}, which means the new branching help reducing the number of conflicts resolved during the planning. There are a few cases where $N_c^{old} < N_c^{new}$, which is due to tie breaking since we do not have a fixed rule to break ties.

We further introduce conflict ratio $(N_c^{old} - N_c^{new})/N_c^{old} \times 100\%$ to compare the number of conflicts. As shown in Fig. 7, the new branching rule is able to reduce up to 70% of the conflicts compared with the old branching rule. The new rule is particularly beneficial with the long task duration.

D. Gazebo Simulation

We run simulation in Gazebo for Scene 3 to execute the joint path planned by CBSS-D. Our simulation settings are $N = 5, M = 10, \tau \in [2, 10]$ as shown in Fig. 8. During the execution, due to the disturbance and uncertainty in the robot motion, additional conflicts may occur when robots execute their paths. We thus implement a management system to monitor the position of all robots and coordinate their motion, by taking advantage of TPG in a similar way as described in TPG-D. Specifically, a TPG is first created based on the planned paths by CBSS-D. When executing the path, nodes in TPG that has not precedence requirements (i.e., satisfying the conditions as described in TPG-D) are deleted from the TPG and are sent to the robots for execution. By

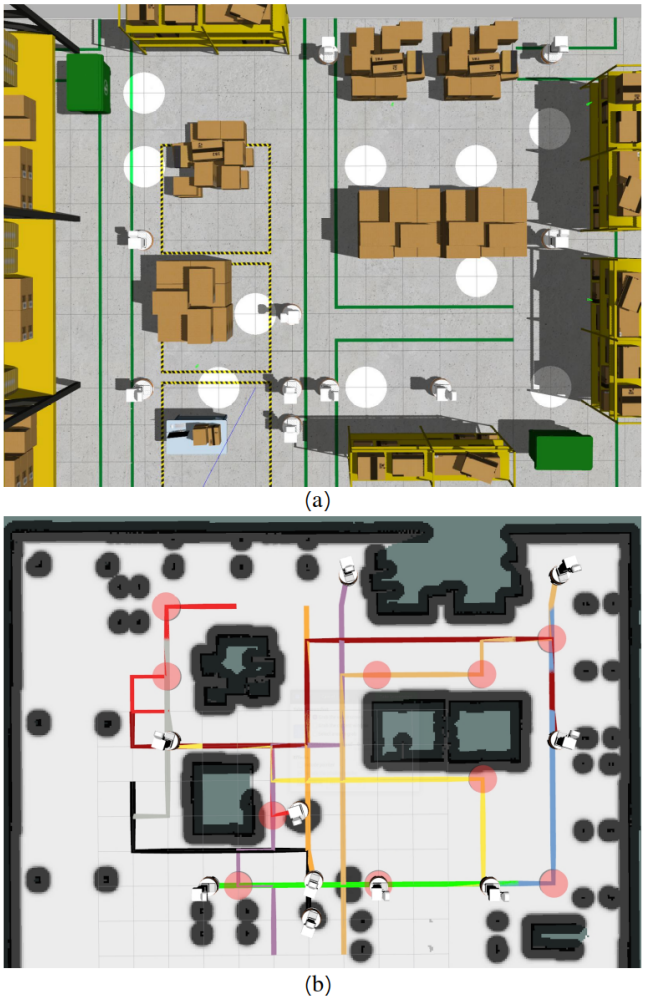

Fig. 8. Simulation using Gazebo and path visualization with Rviz of Scene 3. (a) Gazebo simulation of a warehouse, multiple robots and target tasks (marked by white disks). (b) Rviz visualization of robots, joint path generated by CBSS-D and target tasks (marked by red disks).

doing so, the robots remain collision-free along their paths, even if a robot has unexpected delay or the task duration used by the planner mismatches the actual task execution time. We demonstrate the simulation experiment in the multimedia attachment.

VII. Conclusion and Future Work

This article investigates a generalization of MCPF called MCPF-D, where agents execute tasks at target locations with heterogeneous duration. We developed two methods—CBSS-TPG and CBSS-D to handle MCPF-D, analyzed their properties. verified them with simulation with up to 20 agents and 50 targets, and discussed their pros and cons. For future work, we can consider time window constraints on tasks.

References

[1] Kyle Brown, Oriana Peltzer, Martin A. Sehr, Mac Schwager, and Mykel J. Kochenderfer. Optimal sequential task assignment and path finding for multi-agent robotic assembly planning. In *2020 IEEE International Conference on Robotics and Automation (ICRA)*, pages 441–447, 2020.

[2] Horst W. Hamacher and Maurice Queyranne. K best solutions to combinatorial optimization problems. *Annals of Operations Research*, 4:123–143, 1985.

[3] Keld Helsgaun. General k-opt submoves for the lin–kernighan tsp heuristic. *Mathematical Programming Computation*, 1:119–163, 10 2009.

[4] Wolfgang Hönig, Scott Kiesel, Andrew Tinka, Joseph Durham, and Nora Ayanian. Conflict-based search with optimal task assignment. In *Proceedings of the International Joint Conference on Autonomous Agents and Multiagent Systems*, 2018.

[5] Wolfgang Hönig, TK Kumar, Liron Cohen, Hang Ma, Hong Xu, Nora Ayanian, and Sven Koenig. Multi-agent path finding with kinematic constraints. In *Proceedings of the International Conference on Automated Planning and Scheduling*, volume 26, pages 477–485, 2016.

[6] Wolfgang Hönig, Scott Kiesel, Andrew Tinka, Joseph W. Durham, and Nora Ayanian. Persistent and robust execution of mapf schedules in warehouses. *IEEE Robotics and Automation Letters*, 4(2):1125–1131, 2019.

[7] Michael Jünger, Gerhard Reinelt, and Giovanni Rinaldi. The traveling salesman problem. *Handbooks in operations research and management science*, 7:225–330, 1995.

[8] Jiaoyang Li, Pavel Surynek, Ariel Felner, Hang Ma, TK Satish Kumar, and Sven Koenig. Multi-agent path finding for large agents. In *Proceedings of the AAAI Conference on Artificial Intelligence*, volume 33, pages 7627–7634, 2019.

[9] Hang Ma and Sven Koenig. Optimal target assignment and path finding for teams of agents. In *Proceedings of the 2016 International Conference on Autonomous Agents & Multiagent Systems*, pages 1144–1152, 2016.

[10] Paul Oberlin, Sivakumar Rathinam, and Swaroop Darbha. A transformation for a heterogeneous, multiple depot, multiple traveling salesman problem. In *2009 American Control Conference*, pages 1292–1297, 2009.

[11] Paul Oberlin, Sivakumar Rathinam, and Swaroop Darbha. Today's traveling salesman problem. *IEEE Robotics & Automation Magazine*, 17(4):70–77, 2010.

[12] Mike Phillips and Maxim Likhachev. Sipp: Safe interval path planning for dynamic environments. In *2011 IEEE International Conference on Robotics and Automation*, pages 5628–5635. IEEE, 2011.

[13] Zhongqiang Ren, Anushtup Nandy, Sivakumar Rathinam, and Howie Choset. Dms*: Towards minimizing makespan for multi-agent combinatorial path finding. *IEEE Robotics and Automation Letters*, 9(9):7987–7994, 2024.

[14] Zhongqiang Ren, Sivakumar Rathinam, and Howie Choset. Ms*: A new exact algorithm for multi-agent simultaneous multi-goal sequencing and path finding. In *2021 IEEE International Conference on Robotics and Automation (ICRA)*. IEEE, 2021.

[15] Zhongqiang Ren, Sivakumar Rathinam, and Howie Choset. Cbss: A new approach for multiagent combinatorial path finding. *IEEE Transactions on Robotics*, 2023.

[16] Guni Sharon, Roni Stern, Ariel Felner, and Nathan R Sturtevant. Conflict-based search for optimal multi-agent pathfinding. *Artificial Intelligence*, 219:40–66, 2015.

[17] Roni Stern, Nathan Sturtevant, Ariel Felner, Sven Koenig, Hang Ma, Thayne Walker, Jiaoyang Li, Dor Atzmon, Liron Cohen, TK Kumar, et al. Multi-agent pathfinding: Definitions, variants, and benchmarks. *arXiv preprint arXiv:1906.08291*, 2019.

[18] Pavel Surynek. Multi-goal multi-agent path finding via decoupled and integrated goal vertex ordering. In *Proceedings of the International Symposium on Combinatorial Search*, volume 12, pages 197–199, 2021.

[19] Edo S van der Poort, Marek Libura, Gerard Sierksma, and Jack A.A van der Veen. Solving the k-best traveling salesman problem. *Computers & Operations Research*, 26(4):409–425, 1999.

[20] Jingjin Yu and Steven M LaValle. Structure and intractability of optimal multi-robot path planning on graphs. In *Twenty-Seventh AAAI Conference on Artificial Intelligence*, 2013.

[21] Han Zhang, Jingkai Chen, Jiaoyang Li, Brian C Williams, and Sven Koenig. Multi-agent path finding for precedence-constrained goal sequences. In *Proceedings of the 21st International Conference on Autonomous Agents and Multiagent Systems*, pages 1464–1472, 2022.